JOC Article
pubs.acs.org/joc

Synthesis and Regiochemistry of [60]Fullerenyl 2-Methylmalonate Bisadducts and their Facile Electron-Accepting Properties

Ken Kokubo,*[,†,§] Riyah S. Arastoo,[†] Takumi Oshima,[†] Chun-Chih Wang,[‡] Yuan Gao,[‡] Hsing-Lin Wang,[‡] Hao Geng,[§] and Long Y. Chiang*[,§]

[†]*Division of Applied Chemistry, Graduate School of Engineering, Osaka University, Osaka 565-0871, Japan,* [‡]*Physical Chemistry and Spectroscopy Group, Chemistry Division, Los Alamos National Laboratory, Los Alamos, New Mexico 87545, and* [§]*Department of Chemistry, University of Massachusetts, Lowell, Massachusetts 01854*

kokubo@chem.eng.osaka-u.ac.jp; long_chiang@uml.edu

Received April 30, 2010

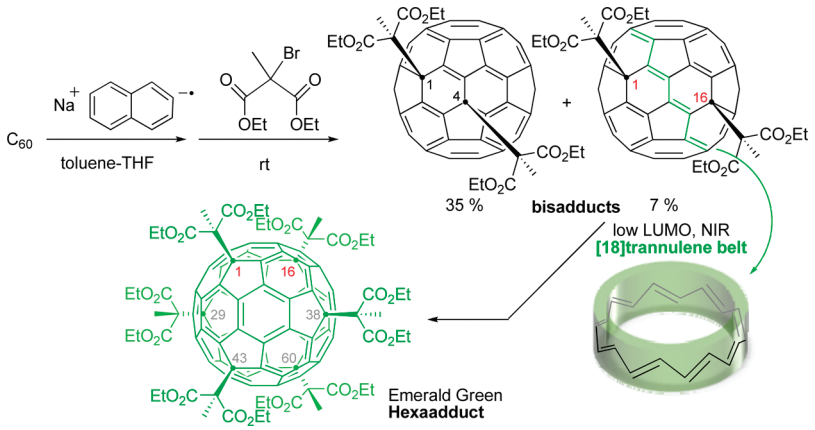

A simple one-pot reaction using *in situ* chemically generated Na-naphthalenide as an electron reductant in the preferential generation of C_{60}^{2-} is described. Trapping of C_{60}^{2-} intermediate with 2 molar equiv of sterically hindered 2-bromo-2-methylmalonate ester afforded two singly bonded fullerenyl bisadducts C_{60}[-CMe(CO_2Et)$_2$]$_2$ in 35% and 7% yield, respectively. The regiochemistry of these two products was determined to be 1,4- and 1,16-bisadducts, respectively, by NMR, UV−vis−NIR, LCMS, and X-ray single crystal structural analysis. The minor 1,16-bisadduct **2** exhibits long wavelength absorption bands in the near-IR region and prominent electron-accepting characteristics as compared with those of the major 1,4-bisadduct and pristine C_{60}. As revealed by DFT calculation, we propose that the origin of these unusual characters of **2** arises from the moiety of [18π]-trannulene, in close resemblance to that of the highly symmetrical emerald green 1,16,29,38,43,60-hexaadduct of C_{60}, EF-6MC$_n$. Accordingly, we anticipate a fast progressive formation of plausible 1,16-bisadduct-like intermediate moieties on a C_{60} cage as the precursor structure leading to the formation of EF-6MC$_n$, by taking the corresponding regiochemistry and electronic properties into account.

Introduction

Effective methods for fullerene functionalization have been investigated over the past decade[1] aiming at the enhancement of solubility and compatibility of C_{60} with the secondary system. Chemical modification of C_{60} also broadens the scope of its participation in electronic and optoelectronic processes for materials utilities, e.g., photovoltaic cells, organic electroluminescence, and nonlinear optical photonics.[2] Thus, the high interest in determining simple, characterizable methods for the preparation of novel well-defined fullerene derivatives persists.

(1) (a) Thilgen, C.; Diederich, F. *Chem. Rev.* **2006**, *106*, 5049–5135. (b) Nakamura, E; Isobe, H. *Acc. Chem. Res.* **2003**, *36*, 807–815. (c) Hirsch, A., Ed.; In *Fullerenes and Related Structures*; Springer: Berlin, 1999; Vol. 199. (d) Diederich, F.; Thilgen, C. *Science* **1996**, *271*, 317–323. (e) Hirsch, A. *Synthesis* **1995**, 895–913.

(2) (a) Guldi, D. M.; Illescas, B. M.; Atienza, C. M.; Wielopolski, M.; Martín, N. *Chem. Soc. Rev.* **2009**, *38*, 1587–1597. (b) Peet, J.; Heeger, A. J.; Bazan, G. C. *Acc. Chem. Res.* **2009**, *42*, 1700–1708. (c) Elim, H. I.; Anandakathir, R.; Jakubiak, R.; Chiang, L. Y.; Ji, W.; Tan, L. S. *J. Mater. Chem.* **2007**, *17*, 1826–1838. (d) Martín, N.; Sánchez, L.; Illescas, B.; Pérez, I. *Chem. Rev.* **1998**, *98*, 2527–2547.

Published on Web 06/04/2010 DOI: 10.1021/jo1007674

SCHEME 1

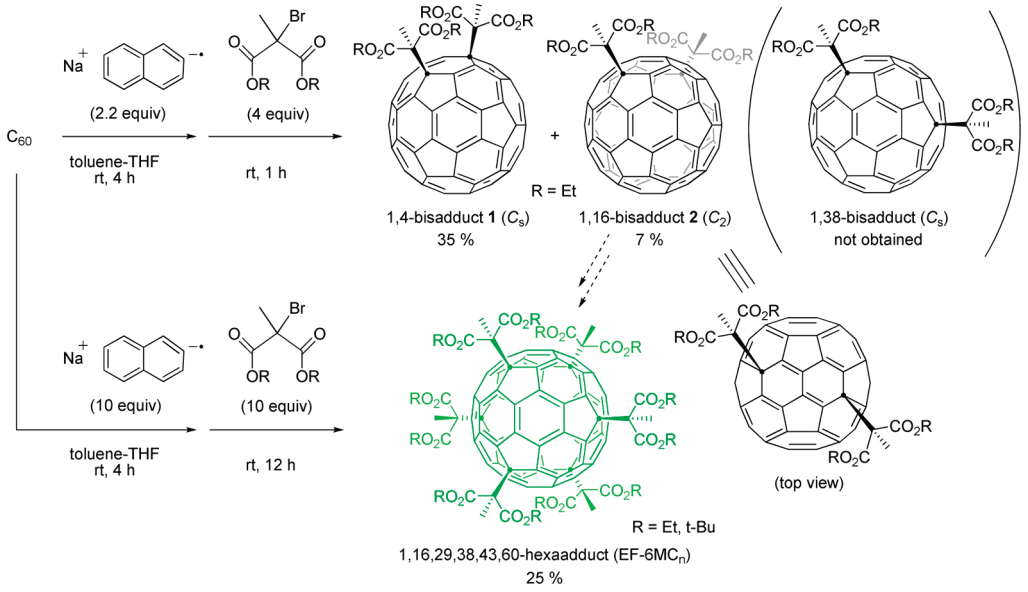

Direct reduction of C_{60} was achieved by transferring one or multiple electrons from metal or organic donors, leading to the generation of corresponding C_{60}^{n-} intermediates,[3] including C_{60}^{2-}, which is a strong electron donor nucleophile in reaction with electrophiles.[4] Such reaction may result in the product of fullerenyl bisadducts. The mechanism of their formation was proposed to follow a sequence of stepwise pathways[5] with an initial step reaction involving C_{60}^{2-} and one alkyl halide molecule, giving the monoalkyl adduct anion, RC_{60}^{-}, via single electron transfer followed by radical coupling. The second step involved the S_N2 reaction of RC_{60}^{-} with the second primary or secondary alkyl halide molecule to afford the corresponding bisadduct derivatives. Chemical generation of C_{60}^{2-} by the thiol donor reduction was plausible in reported methods using either *n*-propanethiol−K_2CO_3[6] or sodium alkanethiolate RS^-Na^+ (R = Me, *n*-Pr, *n*-Bu) as the reagents.[4c−e,7]

Recently we reported the reaction of multianionic C_{60} intermediate (up to C_{60}^{6-})[8] with di(*tert*-butyl) 2-bromo-2-methylmalonate to produce a new class of emerald green fullerenes,[9] giving an example of singly bonded hexaadduct C_{60}[-CMe(CO_2-*t*-Bu)$_2$]$_6$ (EF-6MC$_{4t}$). Here we report the use of sodium naphthalenide as an electron reducing agent for the generation of C_{60}^{2-}, followed by its trapping with diethyl 2-bromo-2-methylmalonate to afford novel fullerenyl 1,4-bisadduct **1**, C_{60}[-CMe(CO_2Et)$_2$]$_2$, in a common 1,4-addition manner along with a minor quantity of 1,16-bisadduct **2** (as a racemic mixture with its enantiomeric 1,29-bisadduct) in an unusual 1,6-addition manner,[10] as shown in Scheme 1. The latter minor bisadduct showed a C_2-symmetry in the molecular structure consistent with 1,16-substituted fullerenyl sp^3 carbon positions that bears a close similarity in regiochemistry, as an adjacent pair of two substituents (1,16 or 1,38), to a partial structure of 1,16,29,38,43,60-hexaadduct EF-6MC$_n$, although the latter C_s-symmetrical 1,38-bisadduct was absent in the same reaction.

Results and Discussion

Experimentally, the reducing agent was prepared by the treatment of naphthalene (78 mg, 0.61 mmol) with sodium metal (> 14 mg, 0.61 mmol) in freshly distilled THF (50 mL) at ambient temperature under N_2 or Ar atmosphere. The solution was stirred until the color changed to dark green. The resulting Na-naphthalenide solution was transferred slowly into the deoxygenated solution of C_{60} (200 mg, 0.28 mmol) in dry toluene (100 mL). The mixture was allowed to stir for 4.0 h at room temperature, followed by the addition of diethyl 2-bromo-2-methylmalonate (281 mg, 1.11 mmol). The reaction was continued for an additional 1.0 h. At the end of reaction, the solvent was removed under reduced pressure, and the residue was purified on a silica gel column using toluene−THF (98:2) as the eluent to afford a mixture of C_{60}[-CMe(CO_2Et)$_2$]$_2$ **1** and **2** as brown solids in a total yield of 42% and a ratio of *ca.* 5:1 based on the HPLC peak area count (5-PBB column, toluene, UV 310 nm). The unreacted C_{60} as confirmed by LCMS was recovered in 20%

(3) Reed, C. A.; Bolskar, R. D. *Chem. Rev.* **2000**, *100*, 1075–1120.
(4) (a) Subramanian, R.; Kadish, K. M.; Vijayashree, M. N.; Gao, X.; Jones, M. T.; Miller, M. D.; Krause, K. L.; Suenobu, T.; Fukuzumi, S. *J. Phys. Chem.* **1996**, *100*, 16327–16335. (b) Kadish, K. M.; Gao, X.; Van Caemelbecke, E.; Hirasaka, T.; Suenobu, T.; Fukuzumi, S. *J. Phys. Chem. A* **1998**, *102*, 3898–3906. (c) Allard, E.; Delaunary, J.; Cheng, F.; Cousseau, J.; Orduna, J.; Garin, J. *Org. Lett.* **2001**, *3*, 3503–3506. (d) Cheng, F.; Murata, Y.; Komatsu, K. *Org. Lett.* **2002**, *4*, 2541–2544. (e) Allard, E.; Delaunary, J.; Cousseau, J. *Org. Lett.* **2003**, *5*, 2239–2242. (f) Zheng, M.; Li, F.; Shi, Z.; Gao, X.; Kadish, K. M. *J. Org. Chem.* **2007**, *72*, 2538–2542.
(5) Fukuzumi, S.; Suenobu, T.; Hirasaka, T.; Arakawa, R.; Kadish, K. M. *J. Am. Chem. Soc.* **1998**, *120*, 9220–9227.
(6) Subramanian, R.; Boulas, P.; Vijayashree, M. N.; D'Souza, F.; Jones, M. T.; Kadish, K. M. *J. Chem. Soc., Chem. Commun.* **1994**, 1847–1848.
(7) Allard, E.; Riviere, L.; Delaunary, J.; Dubois, D.; Cousseau, J. *Tetrahedron Lett.* **1999**, *40*, 7223–7226.
(8) Bhonsle, J. B.; Chi, Y.; Huang, J. P.; Shiea, J.; Chen, B. J.; Chiang, L. Y. *Chem. Lett.* **1998**, 465–466.
(9) (a) Canteenwala, T.; Padmawar, P. A.; Chiang, L. Y. *J. Am. Chem. Soc.* **2005**, *127*, 26–27. (b) Canteenwala, T.; Li, W.; Wang, H. L.; Chiang, L. Y. *Chem. Lett.* **2006**, *35*, 762–763.
(10) (a) Kusukawa, T.; Ando, W. *Angew. Chem., Int. Ed. Engl.* **1996**, *35*, 1315–1317. (b) Kusukawa, T.; Ando, W. *J. Organomet. Chem.* **1998**, *561*, 109–120. (c) Ford, W. T.; Nishioka, T.; Qiu, F.; D'Souza, F.; Choi, J.-P. *J. Org. Chem.* **2000**, *65*, 5780–5184. (d) Maeda, Y.; Rahman, G. M. A.; Wakahara, T.; Kako, M.; Okamura, M.; Sato, S.; Akasaka, T.; Kobayashi, K.; Nagase, S. *J. Org. Chem.* **2003**, *68*, 6791–6794. (e) Tajima, Y.; Hara, T.; Honma, T.; Matsumoto, S.; Takeuchi, K. *Org. Lett.* **2006**, *8*, 3203–3205.

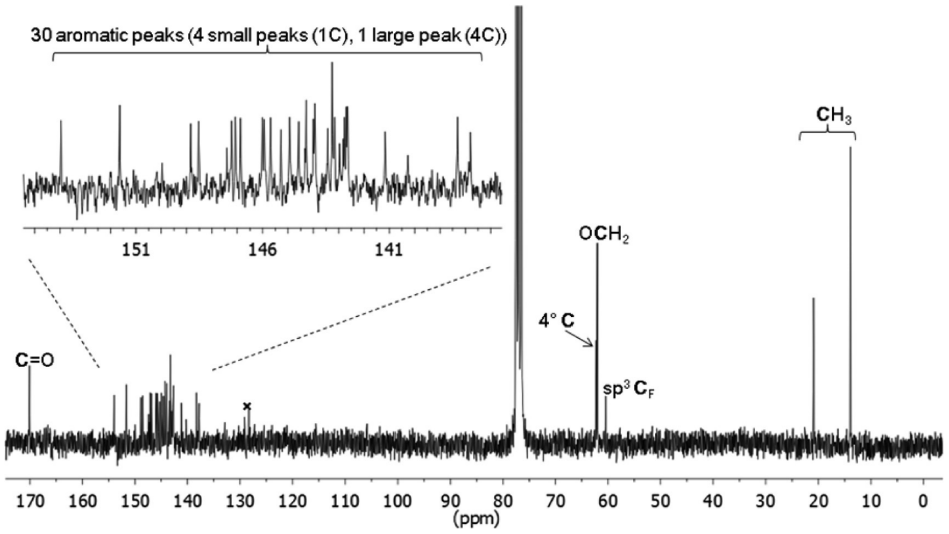

FIGURE 1. ^{13}C NMR spectrum of the bisadduct **1**.

TABLE 1. Reaction of C_{60} with Diethyl 2-Bromo-2-Methylmalonate under Various Conditions

naphthalene (equiv)[a]	anionization time (h)[b]	malonate (equiv)[a]	reaction time (h)[c]	conv (%)[d]	yield **1**/**2** (%)[d,e]
2.2	4	2	72	55	6
2.2	4	10	1	81	35
2.2	2	10	4	76	40
2.2	4	4	1	80	45
10	4	10	1	94	15
10	4	10	12	100	0 (25)[f]

[a]Relative to C_{60} used (0.28 mmol). Sodium was used in excess to naphthalene. [b]Before adding malonate. [c]After adding malonate. [d]Determined by HPLC based on C_{60} used. [e]Combined yield of **1** and **2**. [f]The value in parentheses is the isolated yield of EF-6MC$_2$ hexaadduct.

yield. Further isolation of **1** and **2** was made by using a preparative HPLC equipped with a Buckyprep column with toluene/2-propanol (6:4) as the eluent to afford two products in a yield of 35% and 7%, respectively.

Reaction conditions were roughly optimized as shown in Table 1. To generate the dianion of C_{60} efficiently, 2.2 equiv of naphthalene relative to C_{60} was used. When a nearly equal molar quantity of 2-bromo-2-methylmalonate (2.0 equiv) was used, both the conversion and the yield of bisadducts **1**/**2** remained low (55 and 6%, respectively). By employing an excess amount of malonate (10 equiv), the conversion was increased up to *ca.* 80% and the yield was moderately increased (35−40%). In these conditions, tetraadducts were also obtained along with bisadducts and unreacted C_{60} that may provide the reason why more than 4.0 equiv of malonate is necessary to give the highest yield (45%) and conversion rate. When an excess amount of naphthalene (10 equiv) was applied, the conversion was further increased up to 94% and 100% within the reaction period of 1.0 and 12 h, respectively. However, due to the significant increase of multiadducts, the observed yield of **1**/**2** was reduced to 15% and 0%, respectively. At the end of the reaction period (12 h) under this condition, the greenish hexaadduct, EF-6MC$_2$, was isolated in more than 25% yield.

Structural characterization of **1** and **2** was achieved by various spectroscopic measurements. APPI-LCMS spectra of bisadducts **1** and **2** both showed a weak peak at *m*/*z* 1066, corresponding to the molecular mass ion of $C_{76}H_{26}O_8$, and two clear mass fragmentation peaks at *m*/*z* 721 and 893 corresponding to the loss of a CMe(CO$_2$Et)$_2$ and a [CMe(CO$_2$Et)$_2$]$_2$ moiety, respectively, from the molecular mass ion, however, in different relative peak intensity. In the case of HRMS (MALDI-TOF), the spectrum showed only fragmentation peaks at *m*/*z* 720 and 893 (see Supporting Information). The ^1H NMR spectrum of **1** in $CDCl_3$ basically showed three aliphatic peaks at δ 4.3 (q) and 1.3 (t) for the ethyl group and 2.4 (s) for the methyl group, which was assigned to the diethyl 2-methylmalonate moiety. In more details, the spectrum also displayed two sets of triplets at δ 1.31 and 1.34 (6H, J = 7.3 Hz) and two sets of doublet−quartets at δ 4.31 and 4.32 (2H, J = 14.5 and 7.3 Hz) overlapped with one quartet at δ 4.30 (4H, J = 7.3 Hz). The pattern implies the presence of two sets of carboethoxy groups, indicating the different chemical environment between these two sets out of four ethyl groups, consistent with the plausible C_S or C_2 symmetry. The complex coupling pattern of the peak at δ ~4.3 suggested that one of the sets of carboethoxy groups is suffered from the steric hindrance caused by the neighboring fullerene moiety, while the other carboethoxy group is in a rather far position capable of free rotation. In the case of the minor bisadduct **2**, the corresponding peaks in its ^1H MMR spectrum were essentially the same but slightly shifted to the lower field for the ethyl group and to the higher field for the methyl group, as compared to those of **1**.

More importantly, the ^{13}C NMR spectrum of **1**, as shown in Figure 1, exhibited 30 carbon signals (1 peak of 4C, 25 peaks of 2C, and 4 peaks of 1C) in the range of δ 138−154 for the fullerenyl sp^2 carbons. Two chemical shifts at δ 170.2 and 170.1 were assigned to peaks of two sets of carbonyl carbons. Chemical shift of a tertiary methyl carbon (sp^3) of 2-methylmalonate moiety was found to be 20.9 ppm, based on its peak intensity in a half to that of the terminal ethoxy carbon peak at δ 13.9. One carbon peak at δ 60.4 can be easily assigned to the quaternary carbon of 2-methylmalonate group due to its low peak intensity. The number of fullerenyl carbon peaks revealed a symmetry plane (σ_v) dissecting the molecule with four sp^2 carbons located on the plane. Peaks of these four carbons, each in a reduced signal intensity, were assigned to the

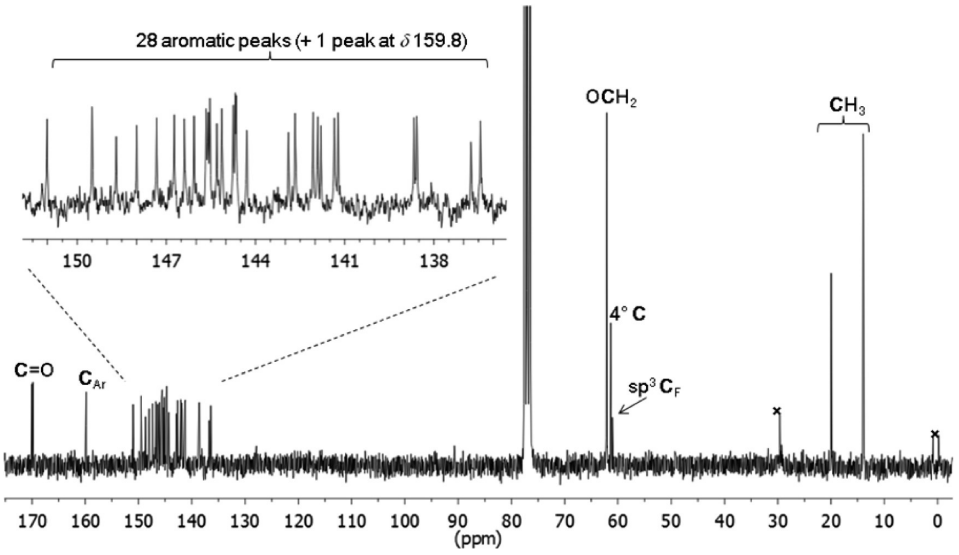

FIGURE 2. ^{13}C NMR spectrum of the bisadduct **2**.

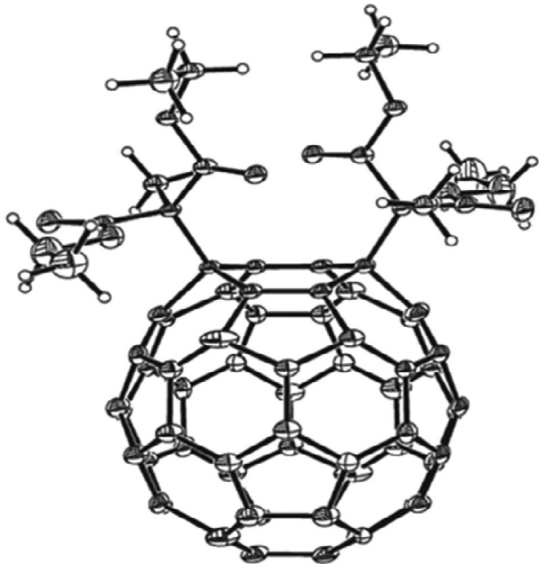

FIGURE 3. ORTEP drawing of the major 1,4-bisadduct **1**.

chemical shift at δ 140.2, 142.8, 143.0, and 144.3, consistent with the C_S symmetrical structure of 1,4-bisadduct. On the other hand, the ^{13}C NMR spectrum of **2**, as shown in Figure 2, showed a spectrum similar to that of **1** except for the aromatic region: the spectrum exhibited 29 carbon signals with almost the same intensity in the range of δ 136−160 for the fullerenyl sp^2 carbons, indicating a C_2 symmetrical structure for this minor 1,16-bisadduct. It is noted that the lowest fielded aromatic peak located apart at δ 159.8 was assigned by DFT simulation as 6- and 15-position carbons which are adjacent to 2-methylmalonate substituted sp^3 carbons at the [5,6]-bond.

Although the calculated ^{13}C NMR patterns in the aromatic region for some bisadduct isomers, based on the DFT calculation, have predicted the structure of the major bisadduct as C_S-symmetrical 1,4- or 1,38-bisadducts,[11] influence of the stereoelectronic effect of substituents as well as the solvent effect may be ignored to obtain the sufficient prediction. Therefore, we carried out the preparation of a single crystal for the X-ray crystal structural analysis. When a mixture of cyclohexane and hexane was used as crystallization cosolvents, we obtained pure single crystals in sufficiently good quality and succeeded in collecting the crystallographic data at 123 K (Figure 3). The crystal included a molecule of cyclohexane in a lattice of the bisadduct. Subsequent structural analysis confirmed this regioisomer as the 1,4-bisadduct **1**, consistent with the ^1H and ^{13}C NMR spectroscopic data. The C_S symmetrical structure at the fullerene moiety has a bisected mirror plane as indicated by its ^{13}C NMR spectrum. However, due to the high steric hindrance at the sp^3 fullerenyl carbon (C_F) region with a very limited degree of freedom for the $\mathbf{C_F}-\mathbf{C}(CH_3)$ bond rotation, the configuration of 2-methylmalonate moieties was found to be oriented in a different C_2 symmetry, not the same C_S symmetry. This interesting feature may make the symmetry prediction complicated for fullerenyl bisadducts having a 2-methylmalonate moiety. Accordingly, two addends of **1** were separated from each other with the closest H−H and O−O interspacing in a short distance of 2.580 and 2.831 Å, respectively.

Several attempts at the crystallization of the minor bisadduct **2** were conducted without success because of its poor crystallinity that may be related to its good solubility as compared with that of **1**. Thus, the regiochemistry of the isomer **2** was determined by the comparison of the UV−vis−NIR spectrum with those of reported structurally known bisadducts reported. The UV−vis spectrum of **1** in THF exhibited four broad absorptions with λ_{max} at 252, 294, 328, and 445 nm (Figure 4). Since the UV spectrum of the 1,4-bisadduct, regardless of the type of addends, typically shows a broad peak around 443−445 nm, optical absorptions of **1** are consistent with this regioisomeric structure.[4e,12]

(11) Kokubo, K.; Thota, S.; Wang, H.-L.; Chiang, L. Y. *J. Macromol. Science, Part A: Pure Appl. Chem.* **2009**, *46*, 1176–1181.

(12) (a) Schick, G.; Kampe, K.-D.; Hirsh, A. *J. Chem. Soc., Chem. Commun.* **1995**, 2023–2024. (b) Nagashima, H.; Terasaki, H.; Saito, Y.; Jinno, K.; Itoh, K. *J. Org. Chem.* **1995**, *60*, 4966–4967. (c) Wang, G.-W.; Murata, Y.; Komatsu, K.; Wan, T. S. M. *Chem. Commun.* **1996**, 2059–2060. (d) Miki, S.; Kitao, M.; Fukunishi, K. *Tetrahedron Lett.* **1996**, *37*, 2049–2052. (e) Zhang, T.-H.; Lu, P.; Wang, F.; Wang, G.-W. *Org. Biomol. Chem.* **2003**, *1*, 4403–4407.

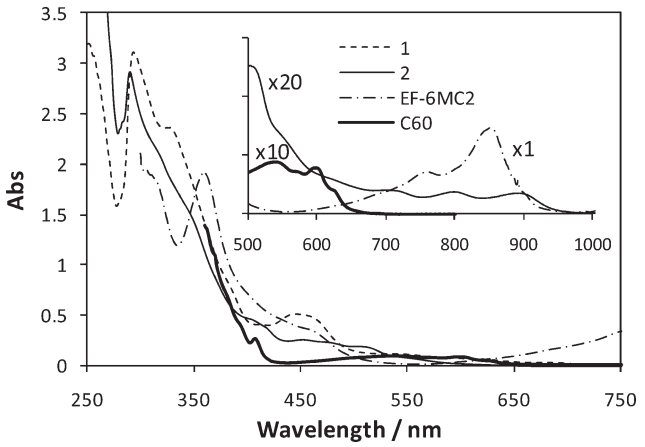

FIGURE 4. UV−vis−NIR spectra of the bisadducts **1** (dotted line), **2** (solid line), and EF-6MC$_2$ (chain line) in THF (0.1 mM). The spectrum of pristine C_{60} (bold line) in toluene (0.1 mM) is also shown for a comparison. The inset is the magnified NIR spectra of the minor bisadduct **2**, EF-6MC$_2$, and C_{60}.

On the other hand, the UV−vis−NIR spectrum of **2** in THF showed the disappearance of a broad peak at 445 nm and the extended absorption to longer wavelengths. As shown in the inset of Figure 4, several absorption bands in weak intensity were observed at 706, 806, and 900 nm in the NIR region. Such a characteristic feature is closely similar to the reported spectrum of the 1,16-bisadduct, where peaks are reported to be 256, 292, 400, 454, 484, 520, 712, 813, and 912 nm,[10c] even though the possibility of the 1,38-bisadduct regioisomer cannot be fully ruled out. Observation of extended absorption up to more than 900 nm for this 1,16-bisadduct **2** is rather rare among many reported [60]fullerene derivatives (including pristine C_{60} as shown in Figure 4 as a comparison), whereas the 1,16,29,38,43,60-hexaadduct (EF-6MC$_n$) also showed a strong absorption at 850 nm as shown in Figure 4.[9a] Since the substituted positions at C(1) and C(16) are common between the structure of **2** and EF-6MC$_n$, the all-*trans* [18π]-trannulene moiety existing in these fullerene derivatives may give the reason for the characteristic similarity in their NIR-absorption characteristics (Figure 5).[13,14]

Structural characterization for the minor bisadduct **2** was also carried out by the comparison of its relative energy stabilization with other regioisomers via semiempirical computational technique. Accordingly, the heat of formation, ΔH_f, of plausible 1,2-, 1,4-, 1,16-, and 1,38-bisadducts were calculated using the MOPAC PM3 method (Figure 6). Among these four regioisomers, the most stable one was found to be the 1,4-bisadduct (1947.4 kJ mol^{-1}; the major product **1**) with the second for the 1,16-bisadduct (1976.3 kJ mol^{-1}; the minor product **2**). The energy difference, $\Delta\Delta H_f$, between 1,4- and 1,16-bisadducts is 28.9 kJ mol^{-1} that is much smaller than $\Delta\Delta H_f$ values calculated for the 1,2- (128.0) and 1,38-bisadduct (726.5). Therefore, our proposed structure of **2** as the 1,16-bisadduct is quite reasonable in addition to the similarity argument of the NIR spectrum, stated above.

Cyclic voltammetric (CV) profiles of **1**, **2**, and C_{60} collected in *o*-dichlorobenzene in the presence of tetra-*n*-butylammonium perchlorate (0.1 M) were shown in Figure 7. The electrochemical data for three reversible reduction waves of **1** and **2** measured between 0.0 and −2.0 V vs Ag/Ag$^+$ were summarized in Table 2. Interestingly, while the first half-wave reduction potential $E_{1red}^{1/2}$ of **1** (−0.92 V) was shifted to a negative potential by 0.12 V relative to that of the pristine C_{60} (−0.80 V) due to the reduction of π-conjugation from 60π to 58π electrons at the fullerenyl cage moiety, the $E_{1red}^{1/2}$ value of **2** (−0.71 V) was found to be shifted to a positive potential by 0.09 V. Since 2-methylmalonate addends on **1** and **2** are the same alkyl groups, this increased electron accepting ability of **2** is not originated from the electron-withdrawing nature of the addend. Such a tendency was also observed in the second ($E_{2red}^{1/2}$) and third ($E_{3red}^{1/2}$) half-wave reduction potentials.

In connection with the previous report the structurally similar 1,16-bisadducts may show similar cyclic voltammograms.[10c] Evidently, the regiochemistry-dependent π-conjugation on the C_{60} cage surface may play an important role in determining the electron-accepting ability of the regioisomer. Kadish et al. have reported that a difference in the first reductive potentials (100 mV) between 1,2-(PhCH$_2$)C_{60} (−0.62 V vs SCE) and 1,4-(PhCH$_2$)C_{60} (−0.52 V) was considered to be large.[4f] In our cases, the observed difference in the potentials between the 1,4-bisadduct **1** and the 1,16-bisadduct **2** (210 mV) is much larger than that value, giving the implication of an unique π-conjugation structure of the latter. Moreover, unsymmetrical electron redox waves were observed with a current intensity for the E_{2red}^{p} wave at −1.44 and −1.28 V in a doubly higher value than those of the corresponding E_{2ox} waves in the redox cycle of **1** and **2**, respectively (Figure 7). This observation bore a close resemblance to a similar unsymmetrical CV profile with higher current intensity for E_{2red}^{p} wave at −1.50 V (vs Fc/Fc$^+$) reported for EF-6MC$_2$.[9b] The phenomena were interpreted by the involvement of disproportionation of $\mathbf{1}^{2-}$ and (EF-6MC$_2$)$^{2-}$ with the neutral **1** and EF-6MC$_2$, respectively, to produce two molecules of $\mathbf{1}^-$ and (EF-6MC$_2$)$^-$ during the reductive cycle. That resulted in an accumulatively higher number of monoanionic intermediate species available for the second electron reduction in the reductive cycle. On the basis of this interpretation, the overall redox wave profiles agreed well with good reversibility and high stability of $\mathbf{1}^{n-}$ with $n \leq 3$.

Higher electron affinity of the 1,16-bisadduct **2** than those of the 1,4-bisadduct **1** and the pristine C_{60} revealed by their cyclic voltammetry was rationalized by the DFT calculation of the HOMO/LUMO energy at B3LYP/6-31G* level of the theory (Figure 8). Two model compounds, 1,4-$C_{60}H_2$ and 1,16-$C_{60}H_2$, were used instead of **1** and **2**, respectively, in order to simplify electronic and steric factors of addends as well as to reduce the calculation time. The order of LUMO energy level in the sequence of 1,4-$C_{60}H_2$ (−3.13) > C_{60} (−3.23) > 1,16-$C_{60}H_2$ (−3.31 eV) is highly related to the

(13) Fokin, A. A.; Jiao, H.; Schleyer, P.; von, R. *J. Am. Chem. Soc.* **1998**, *120*, 9364–9365.

(14) (a) Wei, X.-W.; Avent, A. G.; Boltalina, O. V.; Darwish, A. D.; Fowler, P. W.; Sandall, J. P. B.; Street, J. M.; Taylor, R. *J. Chem. Soc., Perkin Trans. 2* **2002**, 41–46. (b) Burley, G. A.; Fowler, P. W.; Soncini, A.; Sandall, J. P. B.; Taylor, R. *Chem. Commun.* **2003**, 3042–3043. (c) Popov, A.; Senyavin, V. M.; Troyanov, S. I. *J. Phys. Chem. A* **2006**, *110*, 7414–7421. (d) Troshin, P. A.; Koeppe, R.; Susarova, D. K.; Polyakova, N. V.; Peregudov, A. S.; Razumov, V. F.; Sariciftci, N. S. S.; Lyubovskaya, R. N. *J. Mater. Chem.* **2009**, *19*, 7738–7744. (e) Troshin, P. A.; Khakina, E. A.; Zhilenkov, A. V.; Peregudov, A. S.; Troshina, O. A.; Kozlovskii, V. I.; Polyakova, N. V.; Lyubovskaya, R. N. *Eur. J. Org. Chem.* **2010**, 1037–1045.

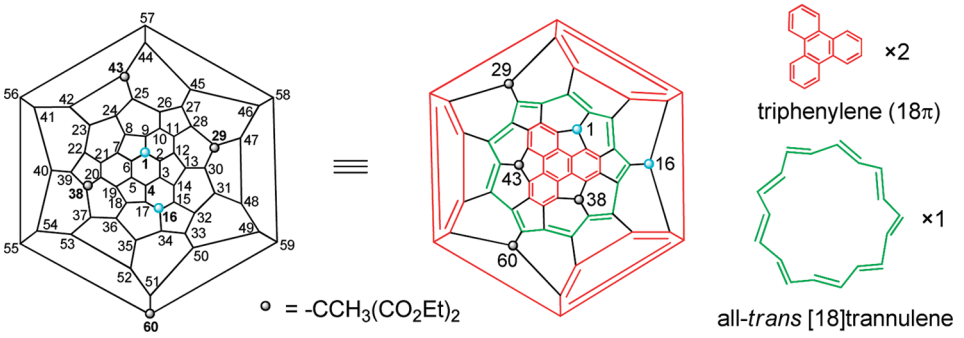

FIGURE 5. Schlegel diagram of the 1,16,29,38,43,60-hexaadduct EF-6MC$_n$ and **2**.

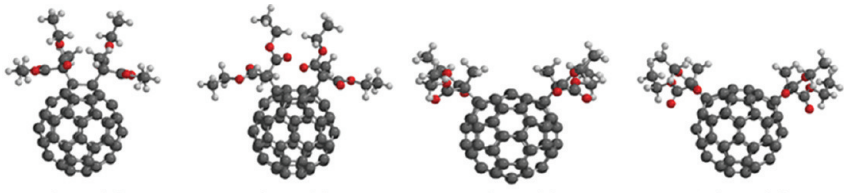

FIGURE 6. Calculated heat of formation ΔH_f for several bisadduct regiostructures of C_{60}[-CMe(CO_2Et)$_2$]$_2$, optimized by the MOPAC PM3 method. The value in parentheses is $\Delta\Delta H_f$ relative to that of the 1,4-bisadduct.

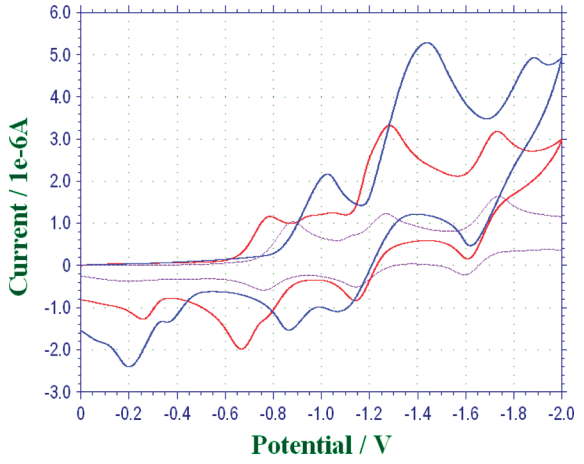

FIGURE 7. Cyclic voltammograms of bisadducts **1** (blue line), and **2** (red line), and C_{60} (purple dotted line).

TABLE 2. Cyclic Voltammetric Data for 1, 2, and C_{60}[a]

	$E^{1/2}$ (V) vs Ag/Ag^+		
	E_{1red}	E_{2red}	E_{3red}
1	−0.92	−1.29	−1.80
2	−0.71	−1.18	−1.66
C_{60}	−0.80	−1.20	−1.66

[a]In 1,2-dichlorobenzene (0.1 mM) in the presence of $(n\text{-Bu})_4N^+(ClO_4)^-$ (0.1 M). Working electrode, Pt; counter electrode, Pt; scan rate, 0.1 V s^{-1}.

order of the first reduction potentials $E_{1red}{}^{1/2}$ as shown in Table 1, in contrast to the order of the HOMO energy level in the sequence of 1,16-$C_{60}H_2$ (−5.36 eV) > 1,4-$C_{60}H_2$ (−5.69) > C_{60} (−5.99). The LUMO energy level of 1,16-$C_{60}H_2$ was 0.08 eV lower than that of C_{60}. The significantly decreased HOMO−LUMO energy gap of 1,16-$C_{60}H_2$ (2.05)

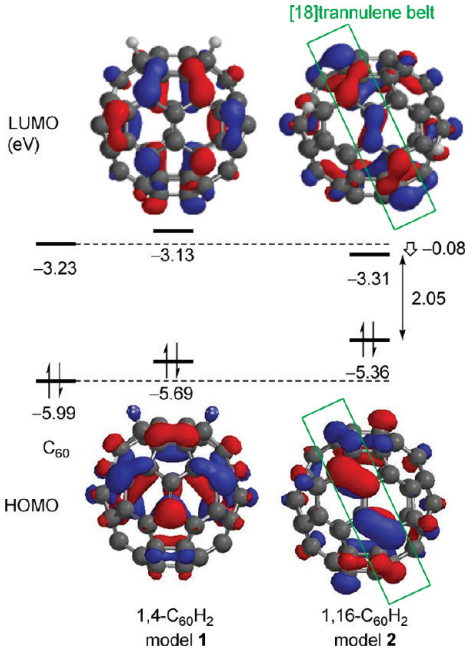

FIGURE 8. Calculated HOMO and LUMO energy (eV) of C_{60}, 1,4-$C_{60}H_2$, and 1,16-$C_{60}H_2$ as the model compound of bisadducts **1** and **2** by the DFT method at B3LYP/6-31G* level of the theory.

as compared with those of 1,4-$C_{60}H_2$ (2.56) and C_{60} (2.76 eV) may be correlated to both analysis results from the NIR absorption spectrum and the nature of all-*trans* [18π]-trannulene moiety[14] of **2**, as discussed in Figure 5, leading to such remarkable electronic properties. Indeed, both calculated HOMO and LUMO energy levels of 1,16-$C_{60}H_2$, as depicted in Figure 8, are mostly located on the [18π]-trannulene belt, whereas those of 1,4-$C_{60}H_2$ and C_{60} are not.

SCHEME 2

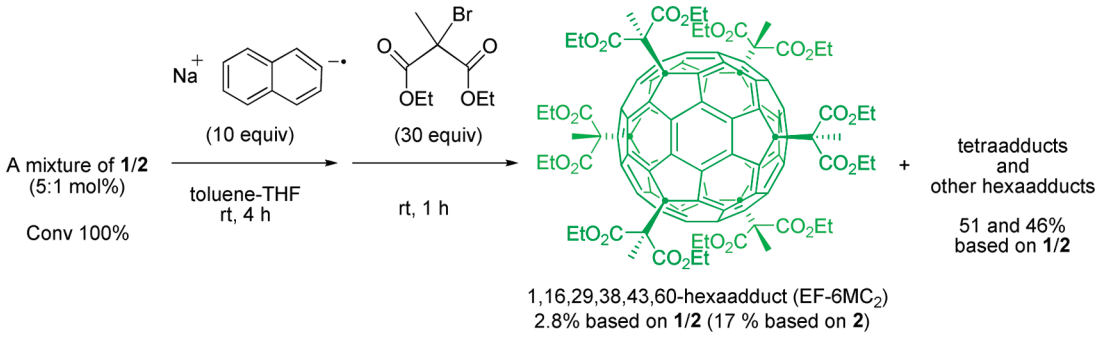

Highly symmetrical molecular structure of EF-6MC$_n$, as shown in Figure 5, was well-resolved by the evidence of its X-ray single crystal structural analysis.[9a] However, the formation mechanism for this unique hexaadduct regioisomer retaining such a high symmetry remains unclear. One explanation for the formation of EF-6MC$_n$ in a good yield (more than 25−30% when optimized) is to experience a faster kinetic rate of hindered malonate attachments on a C_{60} than the negative charge delocalization of C_{60}^{n-}, leading to nearly simultaneous multiple attachments of addends. It is reasonable to correlate this structural feature (the perpendicular relationship of all six addends with each other) to the relative position of all six anions of C_{60}^{6-} in order to minimize the same negative charge repulsion on the cage surface. In principle, any stepwise reaction as those proposed for the formation of 1,2- and 1,4-bisadducts using the reaction of C_{60}^{2-} and alkyl halides[4−7] should result in a great number of unsymmetrical hexaadduct regioisomers during the EF-6MC$_n$ formation reaction.

Accordingly, it is of our interest in making the correlation of the mechanistic formation of **2** as a potential intermediate for the EF-6MC$_2$ chemistry since both bear a similar partial regiostructure in the first two addends. The assumption is plausible owing to the fact that the same reagents were used for the synthesis, except in a different stoichiometric amount. Consequently, both synthetic pathways should proceed through the similar mechanism, reactivity, and kinetics in the early stage of the reaction. Additionally, the 1,4-bisadduct **1** might also be an intermediate product for EF-6MC$_2$ if there is an involvement of rearrangement on the $\mathbf{C_F}-\mathbf{C}(CH_3)$ bond in sigmatropic conjugation with fullerenyl olefins. On the basis of these arguments, we carried out the similar reductive coupling reaction of bisadducts **1** and **2** with 2-bromo-2-methylmalonate in the presence of sodium naphthalenide under the similar condition. This step was intended to give hexaadducts for us to examine whether **1** or **2** can be correlated as the precursors to EF-6MC$_2$ (Scheme 2).

We applied a mixture of **1** and **2** instead of the isolated one because of the limited quantity of isolable minor product **2**. By monitoring with HPLC using 5-PBB column and toluene as the eluent, a mixture of bisadducts (**1**/**2**, 5:1) completely disappeared after 30 min following the addition of the malonate with the appearance of several new peaks. They were assigned to the tetra- and hexaadduct by using the corresponding R_f value, matching with that on a TLC plate [silica gel, R_f = 0.66 for the tetraadduct and 0.61 for the hexaadduct with toluene−THF (9:1) as the eluent], as shown in Figure 9. After a reaction period of 60 min, the HPLC

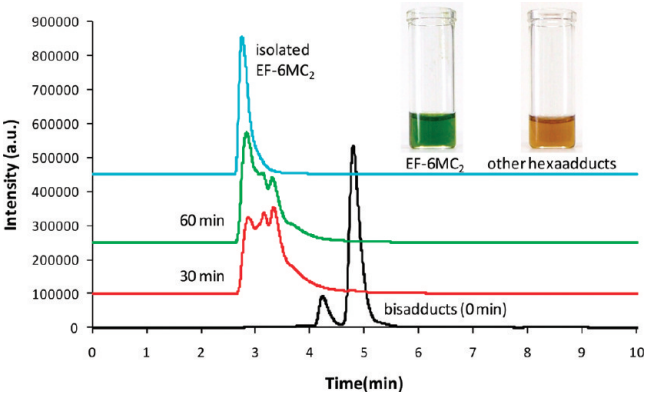

FIGURE 9. HPLC profiles for the reaction of a mixture of bisadducts (0, 30, and 60 min) and the isolated EF-6MC$_2$ (5-PBB, toluene 100%, 1 mL/min, UV 310 nm).

peak of the hexaadduct was slightly increased but remained unchanged even after 3.0 d. By placing the reaction mixture on the TLC plate, a greenish spot assigned to the material of EF-6MC$_2$ overlapped with a brownish spot, which is probably indicative of a mixture of other nonsymmetrical regioisomers of the hexaadduct. Nevertheless, the greenish compound EF-6MC$_2$ from this reaction was isolated by precipitation from the toluene solution upon the addition of hexane, as a poor solvent, and compared with the authentic sample. The yield of EF-6MC$_2$ was only 2.8% based on a mixture of **1**/**2** used and 17% based on the quantity of the minor bisadduct **2** fraction in the starting material. However, this yield is considerably low if the major bisadduct **1** is capable of undergoing sigmatropic rearrangement on the $\mathbf{C_F}-\mathbf{C}(CH_3)$ bond[15] and directly affords the final product of EF-6MC$_2$. Therefore, such fullerenyl anion-induced rearrangement or trotting can be ruled out under the present condition. The direct yield correlation from the minor bisadduct **2** to the product EF-6MC$_2$ seems to be reasonable.

This hypothesis was also verified by the similar reaction employing the isolated bisadduct **1** under the same condition. In this case, no greenish compound EF-6MC$_2$ was detected through the same workup procedure as in the case of a mixture of **1** and **2**. Only a brownish mixture of nonsymmetrical regioisomers of the hexaadduct was obtained along with a large amount of tetraadducts after 30−60 min of reaction (see Supporting Information). These results clearly

(15) "Globe-trotting" hydrogen, but not alkyl addend, have been known: Hirsch, A.; Li, Q.; Wudl, F. *Angew. Chem., Int. Ed. Engl.* **1991**, *30*, 1309–1310.

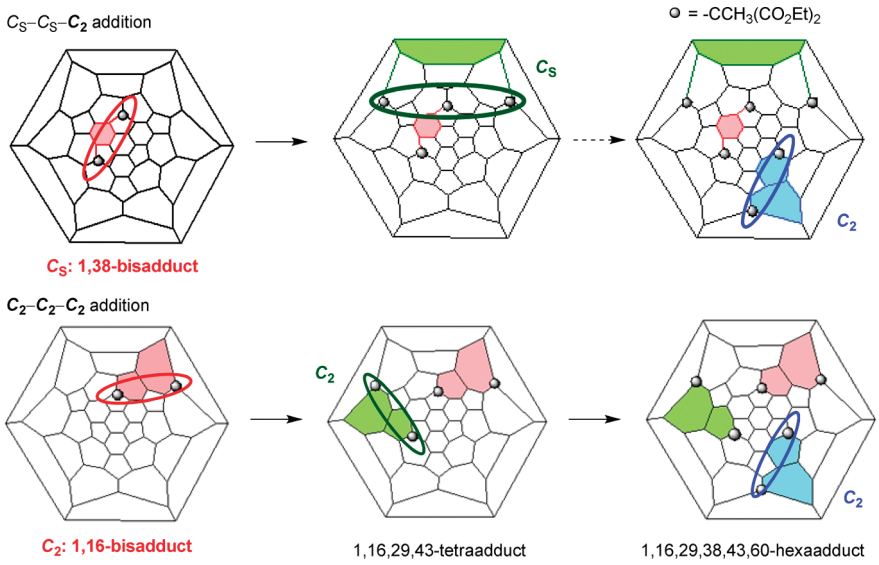

FIGURE 10. Symmetry matching according to a stepwise mechanism for the formation of 1,16,29,38,43,60-hexaadduct EF-6MC$_n$.

implied no structural correlation of **1** to EF-6MC$_2$ through a sequential addition reaction.

In order to examine further the third possibility of the thermally induced rearrangement pathway among different hexaadducts leading to EF-6MC$_2$ as a thermodynamically favorable product, we conducted the isomerization experiment by the treatment of a mixture of nonsymmetrical hexaadduct regioisomers with an excess of sodium naphthalenide (10 equiv) in toluene−THF at room temperature. After 1.0 h or even 3.0 d of reaction, the corresponding greenish spot of EF-6MC$_2$ was not observed on TLC, which supports the former observation on the difficulty in following the rearrangement pathway. It is also noted that a trace amount of the pristine C_{60} was detected by HPLC; presumably, it was indicative of the reverse reaction from the plausible anionic bisadduct species.

Another reason for the argument of **2** to serve as a suitable intermediate for the EF-6MC$_2$ formation is based on its high electronegativity, stated above. The compound **2** formed *in situ* in the reaction mixture should be more suited to the electron reduction by sodium naphthalenide than other intermediate species. This would cause a fast kinetic rate in the disappearance of **2** that could reduce its yield, leading to only a minor product. In the same manner, the 1,38-bisadduct that was not obtained in the present reaction (Scheme 1) may also possibly behave as a much short-lived intermediate toward the formation of EF-6MC$_2$ since the functionalized positions C(1) and C(38) are common between the 1,38-bisadduct and EF-6MC$_2$.[16] However, this possibility is unlikely dominant in the viewpoint of symmetry matching, as demonstrated in Figure 10. Assuming that the hexaadduct is formed by a repeating process of the preferential bisadduct formation, such as the C_2-symmetrical 1,16- or the C_S-symmetrical 1,38-bisadduct, we may consider two possible stepwise pathways in contest toward the formation of highly symmetrical 1,16,29,38,43,60-hexaadduct EF-6MC$_n$ by focusing on the symmetry of regiochemistry. If the first and second steps undergo C_S symmetrical addition to give the 1,38-bisadduct and the subsequent 1,16,29,43-tetraadduct, the third step required is to undergo the C_2 symmetrical addition to attain the desired highly symmetrical regiostructure. In contrast to this unsymmetrical C_S−C_S−C_2 addition path, three repeating processes of the C_2 symmetrical addition giving a C_2−C_2−C_2 addition path can be made via the 1,16-bisadduct to afford the identical EF-6MC$_n$. Such a simple and highly symmetrical circumstance seems to match with the present stepwise mechanism.

As far as the reaction mechanism of C_{60}^{2-} is concerned, C_{60} was known to undergo consecutive electron reductions up to C_{60}^{6-} with the reduction potentials of $E_{1red}^{1/2} = -0.36$ V vs SCE, $E_{2red}^{1/2} = -0.83$, $E_{3red}^{1/2} = -1.42$, $E_{4red}^{1/2} = -2.01$, and $E_{5red}^{1/2} = -2.60$.[17] From the reported value for the reductive potential E_{red}^{p} of naphthalene (Np → Np$^{\bullet-}$) as −2.52 V vs SCE,[18] C_{60}^{4-} (or partially C_{60}^{5-} as well) might be formed in the presence of an excess amount (> 6.0 equiv) of sodium naphthalenide.[19,20] Thus, under the condition to give bisadducts using 2.2 equiv of sodium naphthalenide relative to C_{60}, it is obvious that C_{60}^{2-} is the main anion species formed *in situ*. The reaction mechanism of C_{60}^{2-} with alkyl halide, such as benzyl bromide, have been proposed by Fukuzumi and Kadish et al.[5] to proceed by an electron transfer from C_{60}^{2-} to alkyl halide in the first step followed by the radical coupling between $C_{60}^{\bullet-}$ and R$^{\bullet}$ forming RC_{60}^{-}. The same mechanism can be applied to the present reaction (Figure 11). The last step of the reaction may undergo the

(16) Actually, there are only two possible intermediate bisadducts, C_2-symmetrical 1,16-bisadduct and C_S-symmetrical 1,38-bisadduct, if the neighboring two addends out of six in EF-6MC$_n$ are selected.

(17) Dubois, D.; Kadish, K. M. *J. Am. Chem. Soc.* **1991**, *113*, 7773–7774.

(18) Thornton, T. A.; Ross, G. A.; Patil, D.; Mukaida, K.; Warwick, J. O.; Woolsey, N. F.; Bartak, D. E. *J. Am. Chem. Soc.* **1989**, *111*, 2434–2440.

(19) Other reductants [Fe^{I}(C_5H_5)(C_6Me_6)] (−1.55 V vs SCE; ref 19a) and Li^0 (−3.0 V; ref 19b) were reported to produce C_{60}^{3-} and possibly C_{60}^{6-}, respectively: (a) Bossard, C.; Rigaut, S.; Astruc, D.; Delville, M.-H.; Félix, G.; Février-Bouvier, A.; Amiell, J.; Flandrois, S.; Delhaès, P. *J. Chem. Soc., Chem. Commun.* **1993**, 333. (b) Bausch, J. W.; Prakash, G. K. S.; Olah, G. A.; Tse, D. S.; Lorents, D. C.; Bae, Y. K.; Malhotra, R. *J. Am. Chem. Soc.* **1991**, *113*, 3205–3206.

(20) C_{60}^{2-} and C_{60}^{3-} were also detected in the presence of excess Na in THF: Bhyrappa, P.; Paul, P.; Stinchcombe, J.; Boyd, P. D. W.; Reed, C. A. *J. Am. Chem. Soc.* **1993**, *115*, 11004–11005.

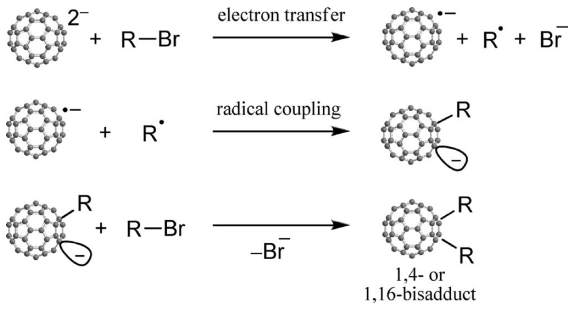

FIGURE 11. Proposed reaction mechanism for the formation of bisadduct $C_{60}R_2$ (R = $CMe(CO_2Et)_2$).

S_N2 substitution while it is difficult for the tertiary 2-bromo-2-methylmalonate.[21] In this case, the second electron transfer can occur from RC_{60}^- to 2-bromo-2-methylmalonate in the same manner as from C_{60}^{2-} followed by a radical coupling process that gives a mixture of bisadducts.[22] On the basis of this mechanism, the regioisomer, 1,4- or 1,16-bisadduct, is determined at the final step; the S_N2 reaction of RC_{60}^- with R−Br or the radical coupling process of $RC_{60}^{\bullet}$ with R$^{\bullet}$. In either case, the 1,4-bisadduct is obviously electronically favorable; however, the 1,16-bisadduct is also formed as a result of the steric hindrance of the bulky addend.

Conclusions

In conclusion, we have demonstrated an efficient method for the preparation of novel fullerenyl 1,4-and 1,16-bisadducts having 2-methylmalonate addends attached on a C_{60} cage via the trapping of C_{60}^{2-} intermediate with highly reactive, sterically hindered 2-bromo-2-methylmalonate esters in yields of 35% and 7%, respectively. The resulting minor 1,16-bisadduct **2** showed several unusual optical absorption bands in the near-IR region up to 950 nm and high electron-accepting ability ($E_{1red}^{1/2}$ = −0.71 V vs Ag/Ag^+) as compared with those of the major 1,4-bisadduct (−0.92 V) and the pristine C_{60} (−0.80 V). As revealed by DFT calculation, we propose that the origin of these unusual characters of **2** arises from the moiety of [18π]-trannulene, in close resemblance to that of the highly symmetrical emerald green 1,16,29,38,43,60-hexaadduct of C_{60}, EF-6MC$_n$. Accordingly, we anticipate a fast progressive formation of plausible 1,16-bisadduct-like intermediate moieties on a C_{60} cage as the precursor structure leading to the formation of EF-6MC$_n$, by taking the corresponding regiochemistry and electronic properties into account.

Experimental Section

General Procedure for the Synthesis of 1,4-C_{60}[$CMe(CO_2Et)_2$]$_2$ (1) and 1,16-C_{60}[$CMe(CO_2Et)_2$]$_2$ (2). Sodium metal (>14 mg, 0.61 mmol or excess) was added to a solution of naphthalene (78 mg, 0.61 mmol) in freshly distilled THF (50 mL) at room temperature under Ar bubbling. After the change of the solution color to dark green, the *in situ* generated sodium naphthalenide solution was transferred slowly into the deoxygenated solution of C_{60} (200 mg, 0.28 mmol) in dry toluene (100 mL). The mixture was stirred for 4.0 h at room temperature, followed by the addition of diethyl 2-bromo-2-methylmalonate (281 mg, 1.11 mmol). After an additional 1.0 h, the solvent and the remaining diethyl 2-bromo-2-methylmalonate were removed under a reduced pressure. The residue was purified on a silica gel column using toluene−THF (98:2) as the eluent to afford a mixture of bisadducts. Preparative HPLC purification of products with a Buckyprep column (eluent, toluene−2-propanol 6:4; flow rate, 1 mL/min; UV, 310 nm) afforded the pure 1,4-C_{60}[$CMe(CO_2Et)_2$]$_2$ **1** as a dark brown solid (104 mg, 35% yield) and 1,16-C_{60}[$CMe(CO_2Et)_2$]$_2$ **2** as a dark brown solid (21 mg, 7% yield).

1,4-Bis(1′,1′-di(carboethoxy)ethyl)-1,4-dihydro[60,I_h]fullerene (1,4-C_{60}[$CMe(CO_2Et)_2$]$_2$) (1). ^{1}H NMR (270 MHz, $CDCl_3$) δ 4.32 (dq, 2H, J = 14.5, 7.3 Hz), 4.31 (dq, 2H, J = 14.5, 7.3 Hz), 4.30 (q, 4H, J = 7.3 Hz), 2.42 (s, 6H), 1.34 (t, 6H, J = 7.3 Hz), and 1.31 (t, 6H, J = 7.3 Hz); ^{13}C NMR (67.5 MHz, $CDCl_3$) δ 170.19 (C=O), 170.05 (C=O), 153.96 (2C), 151.64 (2C), 148.84 (2C), 148.53 (2C), 147.41 (2C), 147.22 (2C), 147.08 (2C), 146.68 (2C), 146.01 (2C), 145.94 (2C), 145.69 (2C), 145.28 (2C), 144.93 (2C), 144.58 (2C), 144.33 (1C), 144.28 (2C), 144.00 (2C), 143.94 (2C), 143.43 (2C), 143.26 (4C), 143.16 (2C), 142.96 (1C), 142.83 (1C), 142.77 (2C), 142.70 (2C), 142.65 (2C), 141.17 (2C), 140.27 (1C), 138.31 (2C), 137.80 (2C), 62.25 (2C, 4°), 62.09 (2C), 62.00 (2C), 60.44 (2C, C_{60}), 20.90 (2C), and 13.89 (4C); UV−vis (THF) λ_{max} 252, 294, 328, and 445 nm; MS (APPI-LCMS) m/z 1066 (M^+), 893, and 721. Crystallographic data for this compound have been deposited at the Cambridge Crystallographic Data Center as supplementary publication # CCDC 772977. The data can be obtained free of charge via www.ccdc.cam.ac.uk/data-request/cif, by emailing data_request@ccdc.cam.ac.uk, or by contacting The Cambridge Crystallographic Data Center, 12 Union Road, Cambridge CB2 1EZ, U.K.; fax: +44 1233336033.

1,16-Bis(1′,1′-di(carboethoxy)ethyl)-1,16-dihydro[60,I_h]fullerene (1,16-C_{60}[$CMe(CO_2Et)_2$]$_2$) (2). ^{1}H NMR (270 MHz, $CDCl_3$) δ 4.43$^-$ 4.22 (m, 8H), 2.25 (s, 6H), 1.33 (t, 6H, J = 7.3 Hz), and 1.29 (t, 6H, J = 7.3 Hz); ^{13}C NMR (67.5 MHz, $CDCl_3$) δ 170.03 (C=O), 169.83 (C=O), 159.83 (2C), 151.02 (2C), 149.50 (2C), 148.69 (2C), 148.00 (2C), 147.33 (2C), 146.74 (2C), 146.39 (2C), 146.07 (2C), 145.67 (2C), 145.59 (2C), 145.53 (2C), 145.30 (2C), 145.14 (2C), 144.75 (2C), 144.68 (2C), 144.65 (2C), 144.29 (2C), 142.90 (2C), 142.67 (2C), 142.06 (2C), 141.91 (2C), 141.80 (2C), 141.35 (2C), 141.23 (2C), 138.67 (2C), 138.58 (2C), 136.75 (2C), 136.43 (2C), 62.10 (4C), 61.36 (2C, 4°), 61.04 (2C, C_{60}), 19.97 (2C), and 13.96 (4C); UV−vis−NIR (THF) λ_{max} 252, 287, 400, 510, 706, 806, and 900 nm; MS (APPI-LCMS) m/z 1066 (M^+), 893, and 721.

Synthesis of 1,16,29,38,43,60-C_{60}[$CMe(CO_2Et)_2$]$_6$ (EF-6MC$_2$) from a Mixture of 1,4- and 1,16-C_{60}[$CMe(CO_2Et)_2$]$_2$ (1/2 = 5:1). Sodium metal (>13 mg, 0.56 mmol or excess) was added to a solution of naphthalene (71.8 mg, 0.56 mmol) in freshly distilled THF (10 mL) at room temperature under Ar bubbling. After the change of the solution color to dark green, the *in situ* generated sodium naphthalenide solution was transferred slowly into the deoxygenated solution of a mixture of C_{60}[$CMe(CO_2Et)_2$]$_2$ (59.7 mg, 0.056 mmol) in dry toluene (40 mL). The mixture was stirred for 4.0 h at room temperature, followed by the addition of diethyl 2-bromo-2-methylmalonate (425 mg, 1.68 mmol). After an additional 1.0 h, the solvent and the remaining diethyl 2-bromo-2-methylmalonate were removed under a reduced pressure and the residue was purified on a silica gel column using toluene−THF (95:5) as the eluent to afford a mixture of hexaadducts. The reprecipitation of the product was carried out by using a mixture of toluene−hexane followed by centrifugation to afford pure 1,16,29,38,43,60-C_{60}[$CMe(CO_2Et)_2$]$_6$ as an emerald green solid (2.8 mg, 2.8% yield based on **1**/**2** and 17% based on **2**).

(21) Bulky alkyl halides, such as *s*-BuI and *t*-BuI, did not undergo the S_N2 reaction with *t*-BuC_{60}^-, although CCl_4 reacted with a small rate constant (ref 5).

(22) Lund, H.; Daasbjerg, K.; Lund, T.; Pedersen, S. U. *Acc. Chem. Res.* **1995**, *28*, 313–319.

Acknowledgment. Research supported by the U.S. Department of Energy, Office of Basic Energy Sciences, Division of Materials Sciences and Engineering, and Grant-in-Aid for Young Scientists (B) (No. 21710109) from MEXT, Japan. We thank Dr. Masato Ohashi (Osaka University) for analyzing of crystallographic data and Dr. Kei Okubo (Osaka University) for measurement of NIR spectrum. The authors at UML are thankful for the financial support of the National Institutes of Health (NIH) under grant no. 1R01CA137108.

Supporting Information Available: APPI-LCMS, MALDI-TOF-HRMS, and ^{1}H and ^{13}C NMR spectra of bisadducts **1** and **2**, HPLC charts for the reaction of bisadduct **1**, ORTEP drawing of **1** (other view), CIF file, and Cartesian coordinates for the calculations. This material is available free of charge via the Internet at http://pubs.acs.org.